

# Evaluation of Wood Species Identification Using CNN-Based Networks at Different Magnification Levels

Khanh Nguyen-Trong\*

Posts and Telecommunications Institute of Technology, Hanoi, Vietnam\*

**Abstract**—Wood species identification (WoodID) is a crucial task in many industries, including forestry, construction, and furniture manufacturing. However, this process currently requires highly trained individuals and is time-consuming. With the recent advances in machine learning and computer vision techniques, automatic WoodID using macro-images of cross-section wood has gained attention. Nevertheless, existing works have been evaluated on ad-hoc datasets with pre-fixed magnification levels. To address this issue, this paper proposes an evaluation of deep learning-based methods for WoodID on multiple datasets with varying magnification levels. Several popular Convolutional Neural Networks, including DenseNet, ResNet50, and MobileNet, were examined to identify the best network and magnification levels. The experiments were conducted on five datasets with different magnifications, including a self-collected dataset and four existing ones. The results demonstrate that the DenseNet121 network achieved superior accuracy and F1-Score on the 20X dataset. The findings of this study provide useful insights into the development of automatic WoodID systems for practical applications.

**Keywords**—Wood species identification; convolutional neural network; ResNet50; DensNet

## I. INTRODUCTION

Wood species identification (WoodID) is a critical aspect in various industries, including forestry, construction, and furniture manufacturing [1], [2]. The identification process involves determining the type of wood based on its unique physical and anatomical characteristics such as growth rings, knots, ray patterns, and texture [3]. In many countries, this process is currently performed manually by forestry experts. The manual process not only poses a challenge in terms of cost and time, but also limits the ability to scale up the identification process to meet the demands of the growing timber industry. This highlights the need for a more automated and accessible approach to WoodID, which could have a significant impact on the efficiency and effectiveness of the forestry industry.

Recently, with the development of machine learning and computer vision techniques, automatic WoodID has received increasing attention. Numerous deep-learning-based methods have been proposed in the literature, which rely on the unique visual characteristics of wood cross-sections [4]. Owing to the widespread availability of low-cost portable digital cameras and stereo microscopes, most of these works used macroscopic images of transverse sections of wood. For example, these studies have been applied to automatic identification of North American hardwood species [5], European tree species [6], Chinese wood species [7], Japanese wood species [8], or

Indonesian commercial wood [9]. They have demonstrated their high accuracy, robustness, and efficiency compared to traditional methods that involve manual feature extraction.

Among the deep learning methods applied for WoodID, Convolutional Neural Network (CNN) based approaches have gained widespread use. Examples of these networks include VGG16 [10], ResNet50 [11], DenseNet [12], and MobileNet [13]. The advantage of using CNNs is that they can automatically identify relevant features in the input images, eliminating the need for manual feature extraction. The availability of large annotated datasets and advancements in hardware and software have further driven the application of CNNs in this field.

These networks have proven their ability to effectively handle the complex macroscopic characteristics of wood and accurately recognize species, as demonstrated, for example, in studies focusing on Pacific and Colombian Amazon wood species [14] and Brazilian flora species [15]. This makes them suitable for practical application in countries where illegal logging is a prevalent issue, such as Vietnam.

Although of the high performance in WoodID, there is no concrete recommendation as to which magnification level is most suitable. These studies applied various magnification levels with different wood species datasets. Besides, the application of these advanced techniques is still limited in many underdevelopment countries, such as Vietnam, where access to resources and data might be scarce. Therefore, there is a need for suitable solutions that consider the best network architecture and magnification level of macroscopic images of wood cross-sections. This would not only aid in better forestry management, but also support efforts to curb illegal logging.

In this study, we evaluated the performance of different convolutional neural networks (CNNs) for WoodID using macro-images of wood cross-sections at various magnification levels. Our objective was to propose a practical and effective CNN-based method for this task. To the best of our knowledge, this is the first attempt to evaluate WoodID on different magnification levels, which has led to the development of a more accurate and practical method not only in Vietnam but also in other countries.

We examined the proposed method's performance on five datasets with different magnifications, including a self-collected dataset of popular imported wood species in Vietnam and four existing ones. The study's results provided insights into the effectiveness of different networks and magnification levels for WoodID.

The remainder of this paper is structured as follows. Section II discusses relevant previous studies. Section III provides the details regarding the evaluated networks. The experimental evaluation is presented in Section IV, and finally, some concluding remarks and a brief discussion are provided in Section V.

## II. RELATED WORKS

Convolutional Neural Networks (CNNs) have been widely used in previous studies for WoodID using images of transverse cross-sections of wood. Popular CNN architectures, such as VGG16, ResNet, DenseNet, and MobileNet, have been proposed and trained on various datasets with different magnification levels. In this study, we focus on the methods that employ two main image levels, namely microscopic and macroscopic transverse cross-sections of wood, to investigate the effectiveness of CNNs for WoodID.

For the first level, previous studies have typically utilized dedicated microscopic devices to capture wood cross-section images [16]. For example, Silva *et al.* [17] presented a method to automatically classify wood species using microscopic images of 77 commercial Central-African timber captured at 25x magnification with an Olympus BX60 microscope and an Olympus UC30 digital camera. Geus *et al.* [18] introduced a wood image dataset consisting of 281 species, with three sets of 20 samples each, corresponding to transverse, radial, and tangential sections, taken on an Olympus SZX7 stereo microscope at 20x magnification. V. Stagno *et al.* [19] conducted a study using NMR to capture samples, including one softwood and four hardwood species. The samples were boiled in distilled water until saturation, and microscopy images were captured using a Zeiss EVO LS10 Environmental Scanning Electron Microscope (ESEM) with EDS. Low vacuum mode was chosen to obtain cross-sectional images of the wood, with a working distance ranging from 4.5 to 5.0 mm and an electron high tension of 20.00 kV. Magnifications of 300x and 1000x were used. The data were acquired using a Bruker Avance-400 spectrometer operating at 9.4 T with a 10 mm micro-imaging probe and XWINNMR and ParaVision 3.2 software.

For macroscopic level studies, digital magnifying glasses connected to smartphones or computers are often used to capture images of wood cross-sections [20]–[22]. These images are taken at different levels of magnification, typically ranging from 10-50X. For example, Saenz *et al.* [23] captured images of 11 forest species using a smartphone with a CMOS sensor and a magnification of 3.9 microns per pixel (about 20x of magnification). The area of interest was 2.5mm x 1.9mm, and lighting was provided by the device.

Lee *et al.* [24] proposed a dataset of 25 species from Yunnan Province, China. The woodblocks were first collected and cut by an electric moto saw into 1 cm<sup>3</sup> pieces and flattened with sandpaper (400 grit, 800 grit, 1000 grit). The images were taken using a mobile phone (OnePlus 3, China) and a 20X magnifying glass, with the original image size being 2048 × 1024 pixels. The central 300 × 300 pixels were selected as the experimental material, as they were clearer and less fuzzy than the other areas. A total of 3000 images were obtained, with which each species including 120 images.

In another study, Filho *et al.* [25] used a Sony DSC T20 camera to capture images of 46 species with a resolution of 150 dpi using artificial lighting. Meanwhile, Sun *et al.* [7] used a mobile phone and a 20X magnifying glass to capture images of 25 wood species with a resolution of 2048x1024 pixels. The images were polished and the middle 300x300 pixels were cropped for clearer results. The dataset was divided into two parts for training and testing, with 2498 images for training and 502 images for testing.

In a study conducted by Souza *et al.* [15] in 2020, 46 Brazilian wood species were collected from the Wood Anatomy and Quality Laboratory (LANAQM) at Federal University of Paraná (UFPR) in Curitiba, Paraná. The transversal surfaces of the samples were sanded with a 120 sandpaper, and macroscopic images were taken using a Zeiss Discovery V 12 stereo microscopes with a resolution of 2080 × 1540 pixels and a 10× magnification. This resulted in a total of 1,901 images.

Additionally, in 2021, de Geus *et al.* [14] introduced a new dataset of 11 Brazilian wood species with high commercial value, with all images being taken from the transverse section using a low-cost portable microscope connected to a smartphone with a resolution of 640 × 480 pixels. The dataset consists of 440 images, with 40 images for each of the 11 species.

Various methods have been proposed in the literature, including traditional machine learning (i.e., k-NN, SVM, ANN) and deep learning (i.e., VGG16, ResNet50, SqueezeNet, DenseNet). Traditional methods require fewer data but rely on handcrafted features, while deep learning models demand more data, but perform automatic feature extraction, resulting in higher accuracy. Among these methods, CNN-based networks have been the most successful for WoodID, with several studies achieving high accuracy rates using different networks such as VGG16, ResNet50, SqueezeNet, and DenseNet. For example, de Geus *et al.* [14] obtained an accuracy of 98.13% with DenseNet, while Lee *et al.* [24] achieved an accuracy of 99.6% with ResNet50. However, each proposed method has specific parameters, such as network architecture and magnification levels, and no concrete recommendation has been made regarding the optimal magnification level for CNN-based WoodID. Therefore, this study aims to evaluate the performance of common CNN-based networks for WoodID using macroscopic images of wood cross-sections at different magnification levels, with a focus on evaluating their practicality for use in Vietnam.

## III. MATERIALS AND METHODS

This section provides a comprehensive overview of the data collection process and the Convolutional Neural Network (CNN) based methods applied in the recognition of wood species. To provide a comparative and objective measure of different wood species, we collected five datasets from different regions, including Vietnam, Pacific and Colombian Amazon, and China. Three popular CNN architectures were examined and evaluated on these datasets, including ResNet50, MobileNetV2, and DenseNet121.

### A. Data Preparation and Collection

The study utilized five datasets, including (i) VN\_26, a self-collected dataset, (ii) WRD\_21, a Southeast Asia wood

TABLE I. THE VN\_26 DATASET (10X, 20X AND 50X)

ID	Family	Scientific Name	ID	Family	Scientific Name
1	Fabaceae	Afzelia africana Smith	14	Fabaceae	Guibourtia coleosperma (Benth.) Leonard
2	Fabaceae	Afzelia pachyloba Harms	15	Fabaceae	Guibourtia demeusei J.Leon.
3	Sapotaceae	Austranella congolensis A.Chev.	16	Fabaceae	Julbernardia pellegriniana Troupin
4	Fabaceae	Berlinia bracteosa Benth.	17	Moraceae	Milicia excelsa (Welw.) C.C.Berg
5	Fabaceae	Brachystegia laurentii (De Wild.) Hoyle	18	Fabaceae	Millettia laurentii De Wild.
6	Fabaceae	Cylicodiscus gabunensis Harms	19	Fabaceae	Monopetalanthus coriaceus Mor.
7	Fabaceae	Dalbergia melanoxylon Guill. et Perr.	20	Rubiaceae	Nauclea diderrichii Merr.
8	Fabaceae	Daniellia thurifera Benn.	21	Fabaceae	Pachyelasma tessmannii (Harms) Harms.
9	Fabaceae	Detarium macrocarpum Harms	22	Fabaceae	Piptadeniastrum africanum Brenan
10	Fabaceae	Distemonanthus benthamianus Baill.	23	Fabaceae	Pterocarpus angolensis DC.
11	Meliaceae	Entandrophragma cylindricum Sprague	24	Fabaceae	Pterocarpus Jacq.
12	Fabaceae	Erythrophleum suaveolens Brenan	25	Fabaceae	Pterocarpus soyauxii Taub.
13	Meliaceae	Guarea cedrata Pellegr.	26	Sapotaceae	Tieghemella africana Pierre

TABLE II. THE WRD\_21 DATASET (20X)

ID	Family	Scientific Name	Number of images	ID	Family	Scientific Name	Number of images
1	Fabaceae	Cassia siamea	28	12	Calophyllaceae	Mesua ferrea	36
2	Lauraceae	Cinnamomum camphora	45	13	Fabaceae	Pterocarpus erinaceus Poir	32
3	Fabaceae	Dalbergia bariensis	96	14	Fabaceae	Pterocarpus indicus	24
4	Fabaceae	Dalbergia cochinchinensis	50	15	Fabaceae	Pterocarpus macrocarpus	91
5	Fabaceae	Dalbergia fusca	59	16	Fabaceae	Pterocarpus santalinus	39
6	Fabaceae	Dalbergia latifolia	36	17	Cupressaceae	Taiwania flousiana	42
7	Fabaceae	Dalbergia odorifera	25	18	Lamiaceae	Tectona grandis	74
8	Fabaceae	Dalbergia oliveri	145	19	Combretaceae	Terminalia myriocarpa	63
9	Ebenaceae	Diospyros ebum	43	20	Combretaceae	Terminalia tomentosa	52
10	Malvaceae	Excentrodendron hsienmu	42	21	Fabaceae	Xylia dolabriformis	54
11	Fabaceae	Intsia spp	50				

dataset published by Sun [26], (iii) BFS\_46, the Brazilian flora species dataset collected in 2020 [15], (iv) BD\_11, the Brazil dataset collected in 2021 [14], and (v) PCA\_11, a dataset containing wood from Pacific and Colombian Amazon region [23]. The datasets include macro-images of wood cross-sections captured by different devices at various magnifications and resolutions. Wood samples were sometimes sanded and polished to improve image quality.

The VN\_26 dataset contains 26 wood species imported to Vietnam, as presented in Table I, with samples collected from different locations on the wood cross-section. We captured the images at three magnification levels (10x, 20x, and 50x) with three different types of microscopes. Each image set has a different resolution and image size. The surfaces of the samples were treated by sanding and polishing before being captured.

The WRD\_21 dataset includes 1,126 macro-images of 21 Southeast Asia wood species [26], as presented in Table II. To create the dataset, the authors polished the cross-section of each wood block using 200 grits and 400 grits sandpaper in sequence and then cleared any remaining dust with a toothbrush. Next, they marked a circular area on the wood block to serve as the fingerprint area, which ensured that the same location for subsequent captures could be chosen. They then used a 20X magnifying glass to acquire an image of the marked area. Finally, the macro-images were captured by a Huawei Honor 8 cellphone.

The BFS\_46 dataset, as presented in Table III, was col-

lected in 2020 and contains 1,901 images of 46 Brazilian flora species with two different sizes (640x480 pixels and 2080x1540 pixels). The wood samples were obtained from the Wood Anatomy and Quality Laboratory (LANAQM) at the Federal University of Paraná (UFPR) in Curitiba, Paraná. They were then sanded with 120 grit sandpaper. The authors used a Zeiss Discovery V 12 stereo-microscope at 10x magnification to capture the macro-images with a resolution of 150 dpi.

The BD\_11 is another Brazilian dataset collected in 2021, consisting of 11 high-commercial-value wood species, as shown in Table IV. The timber samples were not polished; instead, the authors used a pocket knife to cut them to expose the anatomical characteristics. The samples were captured using a low-cost portable microscope connected to a smartphone with a resolution of 640x480 pixels. To account for variance in anatomical characteristics, each species comprises 40 images, with four image samples extracted from 10 different specimens.

The PCA\_11 dataset contains 10,792 images of 11 wood species captured using a digital microscope device at 20x magnification, as presented in Table V. First, timber samples from the Pacific and Colombian Amazon region were aggregated and moistened to increase contrast. Next, they were captured with a digital microscope device at a resolution of 640x480 pixels.

In general, these datasets were collected by capturing images of wood samples using either microscopes or digital

TABLE III. THE BFS\_46 DATASET (10X)

ID	Family	Scientific Name	Number of images	ID	Family	Scientific Name	Number of images
1	Fabaceae	Acrocarpus fraxinifolius Arn.	17	24	Fabaceae	Hymenaea sp. L.	32
2	Araucariaceae	Araucaria angustifolia (Bertol.) Kuntze	55	25	Fabaceae	Hymenolobium petraeum Ducke	28
3	Apocynaceae	Aspidosperma polyneuron Mull. Arg.	20	26	Fabaceae	Hymenolobium sp. Benth.	28
4	Apocynaceae	Aspidosperma Mart. & Zucc.	41	27	Fabaceae	Inga vera Willd.	40
5	Moraceae	Bagassa guianensis Aubl.	52	28	Lauraceae	Laurus nobilis L.	36
6	Rutaceae	Balfourodendron riedelianum (Engl.) Engl.	61	29	Fabaceae	Machaerium paraguayense Hassl.	37
7	Lecythidaceae	Bertholletia excelsa Bonpl.	35	30	Fabaceae	Machaerium sp. Pers.	15
8	Fabaceae	Bowdichia sp. Kunth	68	31	Sapotaceae	Manilkara elata (Allemão ex Miq.) Monach.	39
9	Moraceae	Brosimum parinarioides Ducke	25	32	Meliaceae	Melia azedarach L.	47
10	Meliaceae	Carapa guianensis Aubl.	21	33	Lauraceae	Mezilaurus itauba (Meisn.) Taub. ex Mez	83
11	Lecythidaceae	Cariniana estrellensis (Raddi) Kuntze	36	34	Sapotaceae	Micropholis venulosa (Mart. & Eichler) Pierre	71
12	Meliaceae	Cedrela fissilis Vell.	22	35	Fabaceae	Mimosa scabrella Benth.	30
13	Fabaceae	Cedrelinga cateniformis (Ducke) Ducke	65	36	Fabaceae	Muelleria campestris (Mart. ex Benth.) M.J. Silva & A.M.G. Azevedo	39
14	Boraginaceae	Cordia goeldiana Huber	36	37	Fabaceae	Myroxylon balsamum (L.) Harms	53
15	Lecythidaceae	Couratari sp. Aubl.	41	38	Lauraceae	Nectandra megapotamica (Spreng.) Mez	28
16	Fabaceae	Dipteryx sp. Schreb.	27	39	Lauraceae	Ocotea indecora (Schott) Mez	36
17	Vochysiaceae	Erisma uncinatum Warm.	58	40	Lauraceae	Ocotea porosa (Nees & Mart.) Barroso	46
18	Myrtaceae	Eucalyptus sp. L'Hér.	27	41	Fabaceae	Peltogyne sp. Vogel	60
19	Myrtaceae	Eugenia pyriformis Cambess.	35	42	Pinaceae	Pinus sp. L.	42
20	Rutaceae	Euxylophora paraensis Huber	66	43	Sapotaceae	Pouteria pachycarpa Pires	47
21	Goupiaceae	Goupia glabra Aubl.	32	44	Simaroubaceae	Simarouba amara Aubl.	30
22	Proteaceae	Grevillea robusta A. Cunn. ex R. Br.	48	45	Meliaceae	Swietenia macrophylla King	70
23	Bignoniaceae	Handroanthus sp. Mattos	33	46	Vochysiaceae	Vochysia sp. Aubl	43

TABLE IV. THE BD\_11 DATASET (50X)

ID	Family	Scientific Name	Number of images
1	Lecythidaceae	Allantoma decandra	40
2	Calophyllaceae	Caraipa densifolia	40
3	Lecythidaceae	Cariniana micrantha	40
4	Caryocaraceae	Caryocar villosum	40
5	Moraceae	Clarisia racemosa	40
6	Fabaceae	Dipteryx odorata	40
7	Goupiaceae	Goupia glabra	40
8	Bignoniaceae	Handroanthus incanus	40
9	Malvaceae	Lueheopsis duckeana	40
10	Myristicaceae	Osteophloeum platyspermum	40
11	Sapotaceae	Pouteria caimito	40

TABLE V. THE PCA\_11 DATASET (20X)

ID	Family	Scientific Name	Number of images
1	Anacardiaceae	Camposperma panamensis	823
2	Meliaceae	Cedrela odorata	1128
3	Fabaceae	Cedrelinga cateniformis	1189
4	Boraginaceae	Cordia alliodora	929
5	Myristicaceae	Dialyanthera gracilipes	1100
6	Myrtaceae	Eucalyptus globulus	1105
7	Bignoniaceae	Handroanthus chrysanthus	1106
8	Humiriaceae	Humiriastrum procerum	1001
9	Oleaceae	Fraxinus uhdei	1025
10	Cupressaceae	Cupresus lusitanica	815
11	Pinaceae	Pinus patula	571

cameras. In some cases, the samples were treated by sanding and polishing to improve the image quality. The resolution and size of the images varied among the datasets.

### B. Convolutional Neural Network Architecture

In this study, we focus on deep learning techniques to recognize wood species based on macro-images of wood cross-sections. To achieve this, we utilized several well-known Convolutional Neural Network (CNN) architectures, namely

ResNet [11], DenseNet [12], and Mobilenet [13], which have been widely applied in the field. Each of these models has its strengths and weaknesses. We compared their performance to determine the most effective architecture for WoodID on the studied datasets. In this section, we provide an overview of each network and its specific characteristics.

TABLE VI. RESNET50 ARCHITECTURE

Layer	Type	Output shape	No parameters
1	Input layer	(224,224,3)	-
2	Convolutional	(112,112,64)	1792
3	Max pooling	(56,56,64)	-
4. Res block	Convolutional	(56,56,256)	89600
	Batch normalization	(56,56,256)	1024
	Identity mapping	(56,56,256)	-
5. Res block	Convolutional	(56,56,512)	354944
	Batch normalization	(56,56,512)	2048
	Identity mapping	(56,56,512)	-
6. Res block	Convolutional	(28,28,1024)	1407584
	Batch normalization	(28,28,1024)	4096
	Identity mapping	(28,28,1024)	-
7. Res block	Convolutional	(14,14,2048)	5621248
	Batch normalization	(14,14,2048)	8192
	Identity mapping	(14,14,2048)	-
Average pool	Average pooling	(2048)	-
FC	Fully connected	(1000)	2097000

1) *ResNet50*: ResNet50 is a deep convolutional neural network architecture that was introduced by Microsoft researchers in 2015 [11]. It is part of a family of ResNet models that were designed to address the problem of vanishing gradients in deep neural networks. The authors introduce shortcut connections that allow the gradient signal to bypass some layers during training.

ResNet50 has been widely used in various computer vision tasks, including object detection, image segmentation, and image classification. It has achieved state-of-the-art performance on several benchmark datasets, including ImageNet, which contains over one million images from a thousand different classes. ResNet50 has shown remarkable accuracy and efficiency in recognizing different types of objects, including

wood species, making it a popular choice for many practical applications.

The network consists of a series of convolutional and pooling layers, followed by multiple residual blocks, and finally a global average pooling layer and a fully connected layer, as shown in Table VI.

2) *Densenet*: DenseNet121 is a deep convolutional neural network that was introduced in 2017. It is part of the DenseNet family of models, which is based on the idea of densely connecting each layer to every other layer in a feed-forward fashion [12]. This architecture allows for a deeper and more efficient network that can achieve higher accuracy with fewer parameters compared to traditional architectures like VGG or ResNet.

DenseNet121 consists of 121 layers, with a total of 8.06 million parameters. It has a similar structure to other DenseNet models, where each layer is densely connected to every other layer in a feed-forward fashion. The difference with DenseNet121 is that it uses smaller filters and less dense connections between layers, which allows for better memory usage and faster training. The model also includes skip connections, which help to mitigate the vanishing gradient problem and improve the flow of information throughout the network. Overall, DenseNet121 is a powerful deep learning model that has shown excellent performance in a variety of computer vision tasks, including WoodID.

3) *MobileNet*: MobileNet is a deep learning architecture designed for mobile and embedded devices with limited computational resources. It was introduced by Google in 2017 and has gained significant popularity due to its efficient and lightweight design [13]. The network uses depthwise separable convolutions that separate the spatial and channel-wise convolutions in a standard convolutional layer, as presented in Table VII. This design reduces the number of computations required while maintaining a high level of accuracy.

MobileNet has several variants, including MobileNet v1, v2, and v3. MobileNetV1 was the first version of the architecture and was introduced in 2017. It uses depthwise separable convolutions with a width multiplier, which reduces the number of channels in the network, making it more lightweight. MobileNetV2, introduced in 2018, builds upon the original architecture and introduces several improvements, including linear bottleneck layers and inverted residuals. These changes improve the accuracy and reduce the number of computations required. MobileNetV3, introduced in 2019, focuses on improving the speed and accuracy of the architecture further. It uses a combination of channel and spatial attention modules to improve the network's performance while maintaining its lightweight design. In this study, we evaluated the performance of MobileNetV2.

#### IV. EXPERIMENTS

##### A. Dataset

In this study, we utilized a total of five datasets, of which the VN\_26 dataset was self-collected while the remaining four were obtained from existing sources. For the VN\_26 dataset, wood samples measuring 1 inch (2.54 cm) in size were collected from different locations on the cross-section

TABLE VII. MOBILENET ARCHITECTURE

Layer	Output Shape	Kernel size	Stride
Input	224 × 224 × 3	-	-
Convolution	112 × 112 × 32	3 × 3	2
Depthwise Convolution	112 × 112 × 32	3 × 3	1
Pointwise Convolution	112 × 112 × 64	1 × 1	1
Depthwise Convolution	56 × 56 × 64	3 × 3	2
Pointwise Convolution	56 × 56 × 128	1 × 1	1
Depthwise Convolution	28 × 28 × 128	3 × 3	2
Pointwise Convolution	28 × 28 × 256	1 × 1	1
Depthwise Convolution	14 × 14 × 256	3 × 3	2
Pointwise Convolution	14 × 14 × 512	1 × 1	1
Depthwise Convolution	7 × 7 × 512	3 × 3	2
Pointwise Convolution	7 × 7 × 1024	1 × 1	1
Global Average Pooling	1 × 1 × 1024	-	-
Fully Connected	1000	-	-

of the wood. The collected samples were then processed by surface sanding using sandpaper and polished with 600-grit sandpaper to ensure that the surface texture of each sample was uniform. A small blade was used then to cut this surface. Fig. 1 presents the steps to prepare and collect this dataset. This standardized process of sample preparation allowed us to maintain consistency across the dataset and ensured that the resulting images were of high quality, making them ideal for use.

The dataset was captured using three different types of microscopes at three magnification levels (10x, 20x, and 50x) to obtain a comprehensive set of images. For the 10x dataset, a PCE microscope equipped with a 0.3-megapixel CMOS sensor was used to capture images with a magnification of 10x and a resolution of 640x480 pixels. The 20x dataset was captured using a handheld Dino-Lite electronic microscope, which had a resolution of 1.3 megapixels, a magnification of 20x, and resulted in images of size 1280x1024 pixels. To achieve focus, a distance of 5 cm was maintained between the lens and the sample. Lastly, the 50x dataset was captured using a Wi-Fi Microscope with a magnification ratio of 50x-1000x and resulting in images of size 640x480 pixels.

By using different types of microscopes, we were able to capture images with varying levels of detail, which helped in creating a diverse dataset. The VN\_26 dataset thus obtained serves as a valuable resource for studying wood characteristics. The comprehensive set of images obtained at different magnifications provides ample opportunities to evaluate WoodID at different levels of microscopy.

Table VIII presents an overview of five used datasets. The datasets differ in the number of classes, the total number of images, and the magnification levels, as well as in image resolutions available. For example, the VN\_26 dataset has the highest number of classes and images, with images available at 640x480 and 1280x1024 pixel resolutions. In contrast, the WRD\_21 dataset has fewer classes and images, with images available at a lower resolution of 300x300 pixels. The BFS\_46 dataset has a high number of classes but a relatively low number of images, with images available at two different resolutions of 640 x 480 and 2080 x 1540 pixels. Finally, the BD\_11 and PCA\_11 datasets have similar characteristics, with a lower number of classes but a high number of images available at a resolution of 640 x 480 pixels. To ensure the robustness and generalizability of the models, each dataset was

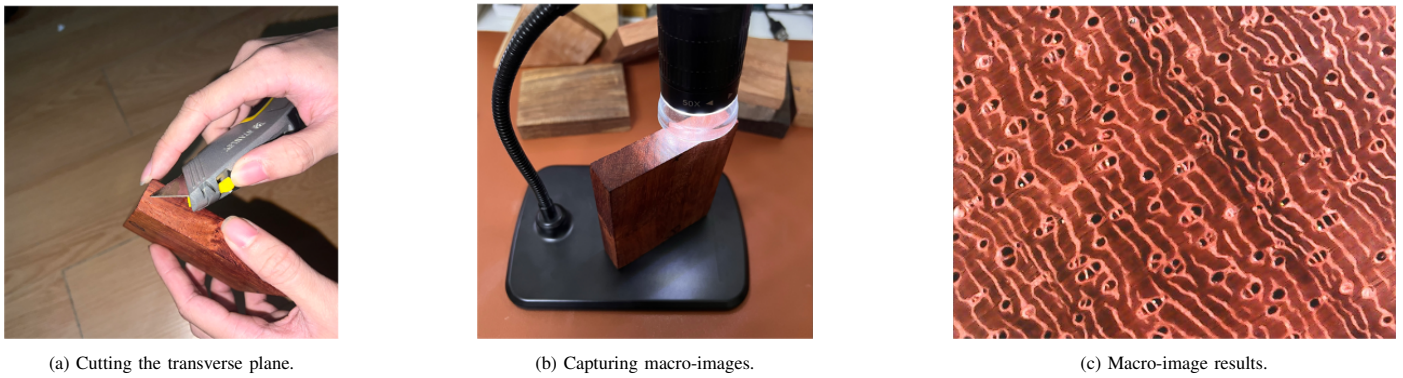


Fig. 1. The VN\_26 dataset preparation and collection.

split into three subsets with a ratio of 70:15:15 for training, validation, and testing.

TABLE VIII. FIVE DATASETS USED IN THIS STUDY

Dataset	Number of classes	Total images	10X	20X	50X	Resolution (pixel)
BFS_46	46	1,901	X			640x480 & 2080x1540
WRD_21	21	1,126		X		300x300
PCA_11	11	10,792		X		640x480
BD_11	11	440			X	640x480
VN_26	26	7,800	X	X	X	640x480 & 1280x1024

### B. Preprocessing

Before training and evaluating the models, we performed several pre-processing steps on the collected dataset. Firstly, the wood identification experts filtered out the poor-quality images, such as blurry and skewed images. The dataset was then re-collected to ensure an adequate number of images for each species (VN\_26). Next, all images were normalized to ensure that the pixel values were within the range of [0, 255]. We then applied techniques to resize them to avoid losing important information.

To enrich the training dataset, we applied various data augmentation techniques such as randomly rotating images within a range of 10 degrees, flipping images randomly horizontally and vertically. These techniques increased the diversity of the training dataset and helped to prevent overfitting of the models.

Finally, we saved the images and their corresponding labels in HDF5 format. HDF5, short for Hierarchical Data Format version 5, is a data model, library, and file format for storing and managing large and complex data. HDF5 provides a flexible and efficient way to store and retrieve large numerical arrays, metadata, and other types of data that are common in scientific computing and data analysis.

Overall, these pre-processing steps played a crucial role in improving the performance of the models and ensuring accurate WoodID. The resulting dataset was of high quality and was well-suited for training deep learning models.

TABLE IX. EXPERIMENTAL SCENARIOS

	Purpose	Network	Dataset
1	Data augmentation evaluation	DenseNet121	PCA_11
2	CNN evaluation on existing datasets	DenseNet121, ResNet50, MobileNetV2	WRD_21, BD_11, BFS_46, PCA_11
3	CNN evaluation on dataset mixed magnifications	DenseNet121, ResNet50, MobileNetV2	VN_26
4	CNN evaluation on dataset with different magnifications	DenseNet121, ResNet50, MobileNetV2	10X, 20X, 50X subsets

### C. Experiment Scenarios

To evaluate the performance of studied deep learning models on various datasets and configurations, we conducted four experiment scenarios, as presented in Table IX. In the first scenario, we evaluated the effect of data augmentation on the PCA\_11 dataset. We trained the DenseNet121 model with an input image size of 224x224 pixels, and a batch size of 32 for 500 epochs using the Adam optimizer with a learning rate of 0.001 and the category cross-entropy loss function. We stopped training if there was no improvement in the validation loss after 200 epochs. Regarding the second scenario, we trained DenseNet121, ResNet50, and MobileNetV2 on four datasets: WRD\_21, BFS\_46, BD\_11, and PCA\_11. The input image size was 224x224 pixels, and we performed training with a batch size of 64 using the Adam optimizer with a learning rate of 0.001. The category cross-entropy loss function was used, and training was stopped if there was no improvement in the model after 200 epochs.

For the third scenario, we trained the same three models on the self-collected dataset, VN\_26, which includes three levels of image magnification. The input image size and other parameters were identical to those used in the first scenario. In the fourth scenario, these four models were separately trained on three subsets of VN\_26, corresponding to the three magnification levels. The same parameters as the previous scenarios were applied, but we stopped training if there was no improvement after 300 epochs.

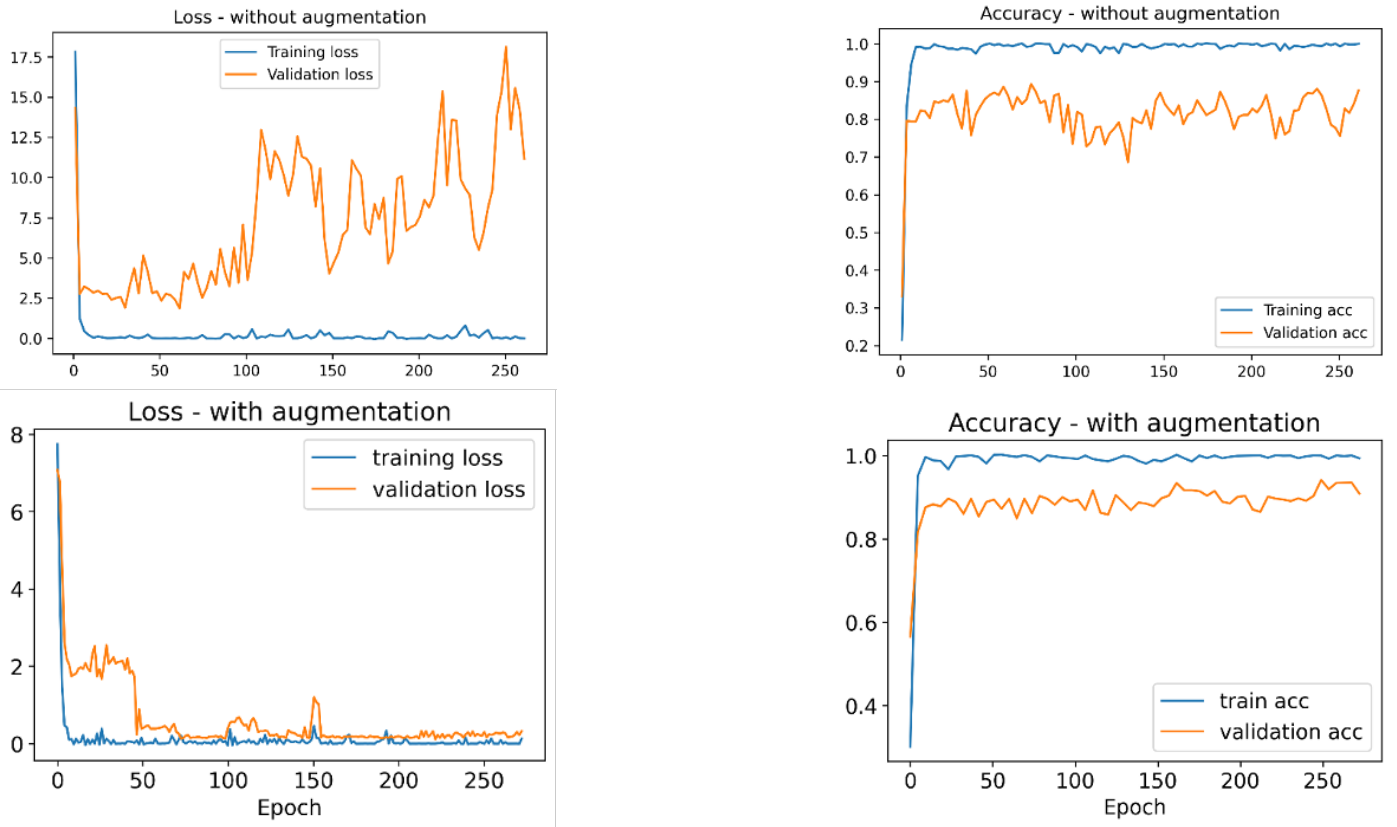


Fig. 2. Experiment 1 – Training loss and accuracy progresses with and without data augmentation.

#### D. Results and Discussion

The obtained results from the first experiment are depicted in Fig. 2, showing the progress of loss and accuracy during the training process on both the non-augmented (the upper plots) and augmented (the lower plots) datasets. It was observed that without data augmentation, the gap between the training and validation accuracy remained large and constant, while the gap between the two loss progresses tended to increase, indicating an overfitting trend. However, with data augmentation, the overfitting was mitigated, as the gap between the two loss progresses was small, and the accuracy gap was reduced. Consequently, the model achieved a higher accuracy of over 95.9% on the validation dataset.

TABLE X. EXPERIMENT 2 - PERFORMANCE OF DEEP LEARNING MODELS ON THE FOUR EXISTING DATASETS

Dataset	Model	Acc	F1-Score	Precision	Recall
BFS_46	Resnet50	87.77%	87.89%	88.35%	87.46%
	MobilenetV2	97.05%	97.08%	97.09%	97.08%
	Densenet121	98.21%	98.22%	98.23%	98.21%
WRD_21	Resnet50	76.12%	76.43%	80.27%	73.28%
	MobilenetV2	94.34%	94.67%	94.52%	94.85%
	Densenet121	97.11%	97.56%	97.39%	97.55%
BD_11	Resnet50	87.24%	63.67%	80.23%	53.91%
	MobilenetV2	96.82%	96.43%	96.16%	96.45%
	Densenet121	97.26%	97.54%	97.37%	97.29%
PCA_11	Resnet50	87.36%	76.15%	80.86%	73.23%
	MobilenetV2	96.25%	96.34%	96.23%	96.25%
	Densenet121	97.78%	97.86%	97.35%	97.66%

Table X presents the outcomes of the second experiment,

demonstrating that all models achieved high accuracy levels in most cases. The best accuracy of 98.21% was achieved by DenseNet121 models on the BR\_46 dataset, whereas the Resnet50 model achieved lower accuracy levels ranging from 76% to 87% across different datasets. The F1-Score had a similar trend to accuracy. Regarding precision and recall, all models showed high values, indicating a good ability to identify true positives and true negatives correctly. Notably, MobileNetV2 and DenseNet121 models consistently achieved higher precision and recall values than the Resnet50. Overall, the results suggest that the choice of the CNN model can significantly affect the accuracy and performance of WoodID, with DenseNet121 being the most effective models in this study. Additionally, the dataset choice could impact the model's performance, with some datasets being more challenging to classify than others.

For the third experiment, the results presented in Table XI show that all three models achieved high accuracy levels, ranging from 86.13% to 99.53%. Notably, the DenseNet121 model outperformed the other two models, achieving the highest accuracy, F1-Score, precision, and recall, with a score of 99.52% and 99.53% in all metrics. In contrast, the MobileNetV2 and ResNet50 models obtained lower accuracy levels, with MobileNetV2 performing better than ResNet50. To gain further insights, we also examined the loss and accuracy progress of the MobileNetV2 and DenseNet121 models, as shown in Fig. 3. The accuracy of both models increased steadily, with validation accuracy closely following the training accuracy. The loss progresses of MobileNetV2 showed a

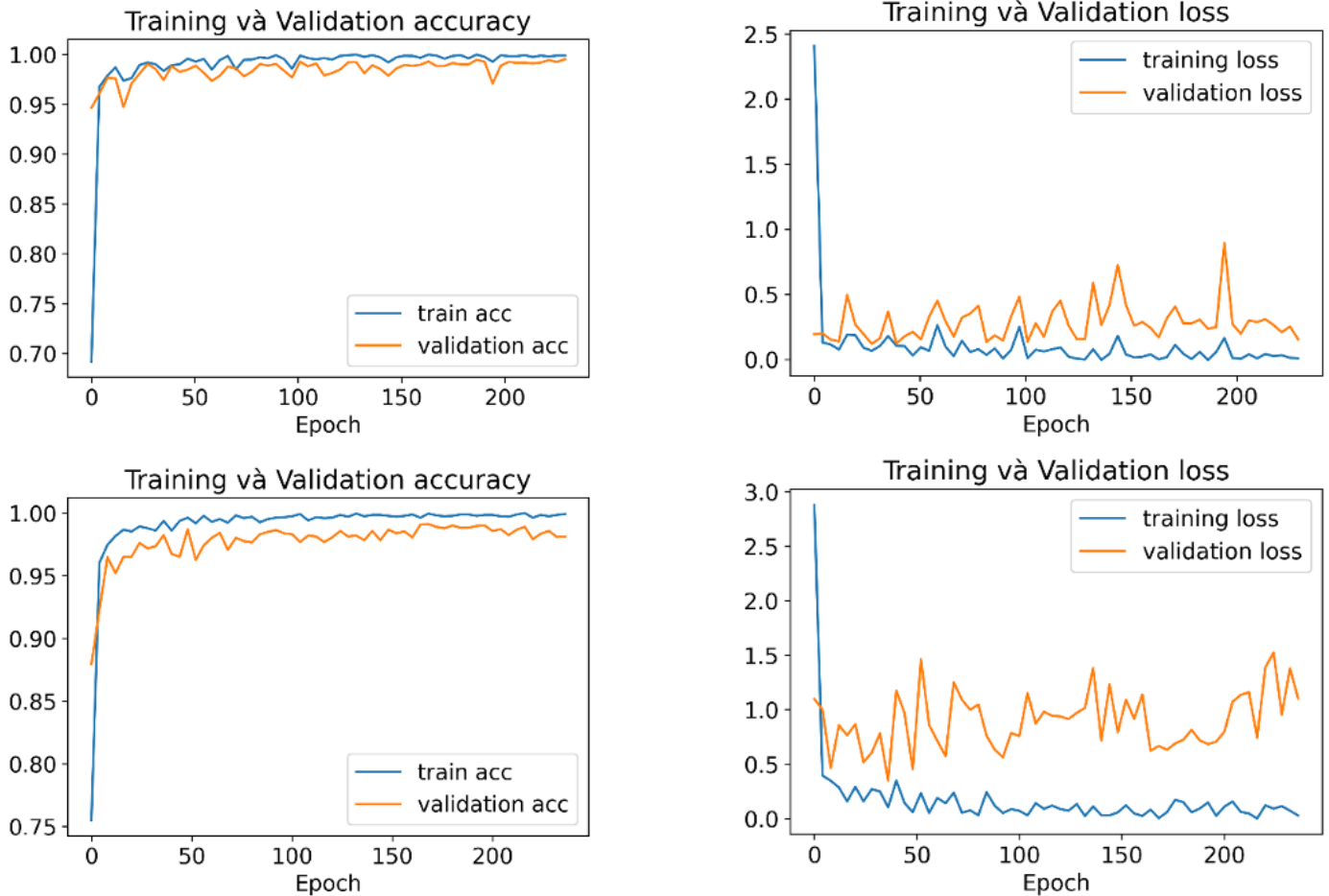


Fig. 3. Exp3: Training loss and accuracy progresses of DenseNet121 (the upper images) and MobileNetV2 (the lower images) on the VN\_26 dataset.

slight overfitting trend, while those of DenseNet121 tended to decrease and approached the training loss progress. It means that MobileNetV2 may not generalize well to new data, while DenseNet121 has a better generalization ability in the model. Overall, the results suggest that DenseNet121 is the most effective model for WoodID on the VN\_26 dataset, achieving high accuracy and generalization ability. These findings are consistent with previous studies that have shown the effectiveness of DenseNet121 on other datasets.

TABLE XI. EXPERIMENT 3 - PERFORMANCE OF DEEP LEARNING MODELS ON THE ALL VN\_26 DATASET

Model	Acc	F1-Score	Precision	Recall
Resnet50	86.13%	86.30%	85.08%	87.34%
MobilenetV2	98.13%	98.15%	98.11%	98.10%
<b>Densenet121</b>	<b>99.52%</b>	<b>99.53%</b>	<b>99.53%</b>	<b>99.53%</b>

The fourth experiment aimed to evaluate the performance of the three CNN models on the three magnification subsets of the VN\_26 dataset, including X10, X20, and X50. As shown in Table XII, all three models achieved high accuracy levels across all magnification levels. Specifically, DenseNet121 outperformed the other models in all metrics, reaching an accuracy of from 99.12% to 99.89% in all levels.

At the X10 magnification level, Densenet121 achieved

TABLE XII. EXPERIMENT 4 – PERFORMANCE OF DEEP LEARNING MODELS ON THE DIFFERENT MAGNIFICATION LEVELS

X levels	Model	Acc	F1-Score	Precision	Recall
X10	Resnet50	86.11%	86.14%	86.61%	85.72%
	MobilenetV2	98.91%	98.82%	98.80%	98.15%
	<b>Densenet121</b>	<b>99.56%</b>	<b>99.61%</b>	<b>99.50%</b>	<b>99.52%</b>
X20	Resnet50	84.64%	83.75%	84.17%	83.34%
	MobilenetV2	99.67%	99.68%	99.68%	99.68%
	<b>Densenet121</b>	<b>99.89%</b>	<b>99.89%</b>	<b>99.89%</b>	<b>99.89%</b>
X50	Resnet50	85.70%	85.90%	86.60%	85.30%
	MobilenetV2	98.32%	98.13%	98.35%	98.31%
	Densenet121	99.12%	99.15%	99.20%	99.14%

the highest accuracy, F1-Score, precision, and recall, with values of 99.56%, 99.61%, 99.50%, and 99.52%, respectively. Meanwhile, at the X20 magnification level, Densenet121 significantly outperformed the other two models, achieving the highest accuracy of 99.89% across all metrics. At the X50 magnification level, all three models achieved high accuracy levels, with Densenet121 and MobilenetV2 achieving the highest accuracy of 99.12% and 98.32%, respectively.

Furthermore, the loss and accuracy progress of all three models were analyzed, and no overfitting trends were observed, as shown in Fig. 4. This indicates that the models were able to generalize well to the test data and were not simply



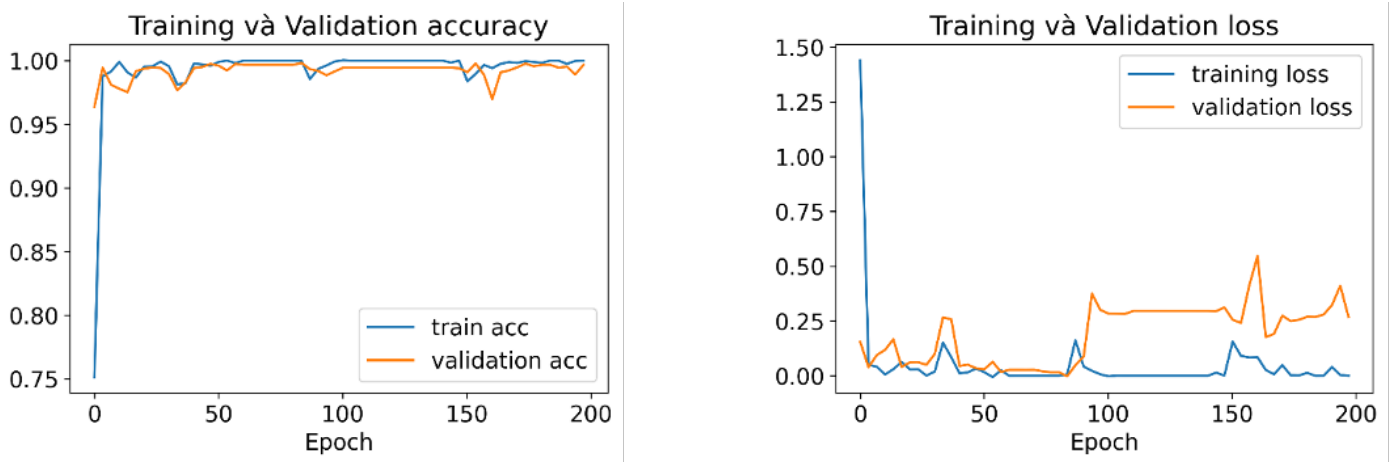


Fig. 4. Exp4: Training loss and accuracy progresses of DenseNet121 on the X20 subset.

memorizing the training data. Among the three magnification levels tested, X20 was found to be the best magnification level for WoodID, with all three models achieving the highest accuracy levels at this magnification. This may be due to the balance between image resolution and information content, which is important for accurately identifying wood species.

TABLE XIII. PERFORMANCE COMPARISON BETWEEN MOBILENETV2 AND DENSENET121

Model	Total parameters	Predicted time (s)	Acc	F1_score
DenseNet121	7,589,451	4.15	100%	100%
MobileNetV2	2,947,915	1.97	99.6%	99.6%

Table XIII provides a comparison between DenseNet121 and MobileNetV2 models. DenseNet121 has a larger number of parameters, which results in a longer predicted time. However, it achieves a higher accuracy and F1 score. On the other hand, MobileNetV2 has fewer parameters, leading to a faster predicted time, but slightly lower accuracy and F1 score. Based on the differences in the number of parameters and predicted time, MobileNetV2 is a suitable choice for low-configuration devices where computational resources are limited. Meanwhile, DenseNet121 can be used for powerful servers where accuracy is critical, and the model's complexity is not a concern.

Overall, we observed that higher magnifications lead to higher accuracy up to a certain level, after which the accuracy can decrease. Specifically, the results indicated that the 20x magnification level outperformed the 10x level in terms of accuracy, F1-Score, precision, and recall for all three models: ResNet50, MobileNetV2, and DenseNet121. This suggests that a higher magnification level provides more information, which allows for better differentiation of wood species.

However, the performance of the models on the 50x magnification level was worse than the 20x and 10x levels. This can be explained by the fact that the 50x level is too close, which can miss important information about the wood structure. At this magnification level, it is possible that the image captures only a small portion of the wood, which may not be representative of the entire sample.

Therefore, our study suggests that the optimal magnification level for wood species recognition is 20x, as it provides enough information without sacrificing accuracy due to the over-saturation of details.

## V. CONCLUSION

In conclusion, this study evaluated the performance of three popular CNN models, MobileNetV2, ResNet50, and DenseNet121, for wood species identification using datasets at different magnification levels. The results demonstrated that data augmentation and the choice of CNN model significantly affected the accuracy and generalization ability of wood species identification. Moreover, the datasets used in the study also impacted the model's performance, with some datasets being more challenging to classify than others.

Overall, the DenseNet121 model consistently outperformed the other models in terms of accuracy, F1-Score, precision, and recall, making it the most effective model for wood species identification across all experiments. Furthermore, the study found that X20 magnification level was the best magnification level for wood species identification, as all three models achieved the highest accuracy levels at this magnification level.

Future work in this area may involve further exploring the impact of different data augmentation techniques on wood species identification. Additionally, the study may be extended to include a larger and more diverse dataset to further test the robustness of the CNN models. Moreover, future research could investigate the transfer of learning techniques for wood species identification to reduce the computational cost and increase the efficiency of the training process. Lastly, it is worth considering the combination of different image processing techniques, such as texture analysis and segmentation, with CNN-based networks to further improve the accuracy of wood species identification.

## ACKNOWLEDGMENT

This work was supported by the 2023 research fund of Posts and Telecommunications Institute of Technology (PTIT), Hanoi, Vietnam.

REFERENCES

- [1] I. Topalova, "Recognition of similar wooden surfaces with a hierarchical neural network structure," *International Journal of Advanced Research in Artificial Intelligence*, vol. 4, no. 10, 2015.
- [2] T. H. Chun, U. R. Hashim, S. Ahmad, L. Salahuddin, N. H. Choon, and K. Kanchymalay, "Efficacy of the image augmentation method using cnn transfer learning in identification of timber defect," *International Journal of Advanced Computer Science and Applications*, vol. 13, no. 5, 2022.
- [3] R. Shmulsky and P. D. Jones, *Forest products and wood science: an introduction*. John Wiley & Sons, 2019.
- [4] S.-W. Hwang and J. Sugiyama, "Computer vision-based wood identification and its expansion and contribution potentials in wood science: A review," *Plant Methods*, vol. 17, no. 1, pp. 1–21, 2021.
- [5] D. J. Verly Lopes, G. W. Burgreen, and E. D. Entsminger, "North american hardwoods identification using machine-learning," *Forests*, vol. 11, no. 3, p. 298, 2020.
- [6] A. Fabijańska, M. Danek, and J. Barniak, "Wood species automatic identification from wood core images with a residual convolutional neural network," *Computers and Electronics in Agriculture*, vol. 181, p. 105941, 2021.
- [7] Y. Sun, Q. Lin, X. He, Y. Zhao, F. Dai, J. Qiu, and Y. Cao, "Wood species recognition with small data: a deep learning approach," *International Journal of Computational Intelligence Systems*, vol. 14, no. 1, pp. 1451–1460, 2021.
- [8] T. Fathurahman, P. Gunawan, E. Prakasa, J. Sugiyama, *et al.*, "Wood classification of japanese fagaceae using partial sample area and convolutional neural networks," *Journal of the Korean Wood Science and Technology*, vol. 49, no. 5, pp. 491–503, 2021.
- [9] M. Arifin, B. Sugiarto, R. Wardoyo, Y. Rianto, *et al.*, "Development of mobile-based application for practical wood identification," in *IOP Conference Series: Earth and Environmental Science*, vol. 572, p. 012040, IOP Publishing, 2020.
- [10] K. Simonyan and A. Zisserman, "Very deep convolutional networks for large-scale image recognition," 2015.
- [11] K. He, X. Zhang, S. Ren, and J. Sun, "Deep residual learning for image recognition," 2015.
- [12] G. Huang, Z. Liu, L. Van Der Maaten, and K. Q. Weinberger, "Densely connected convolutional networks," in *Proceedings of the IEEE conference on computer vision and pattern recognition*, pp. 4700–4708, 2017.
- [13] A. G. Howard, M. Zhu, B. Chen, D. Kalenichenko, W. Wang, T. Weyand, M. Andreetto, and H. Adam, "Mobilenets: Efficient convolutional neural networks for mobile vision applications," *arXiv preprint arXiv:1704.04861*, 2017.
- [14] A. R. de Geus, A. R. Backes, A. B. Gontijo, G. H. Albuquerque, and J. R. Souza, "Amazon wood species classification: a comparison between deep learning and pre-designed features," *Wood Science and Technology*, vol. 55, pp. 857–872, 2021.
- [15] D. V. Souza, J. X. Santos, H. C. Vieira, T. L. Naide, S. Nisgoski, and L. E. S. Oliveira, "An automatic recognition system of brazilian flora species based on textural features of macroscopic images of wood," *Wood Science and Technology*, vol. 54, no. 4, pp. 1065–1090, 2020.
- [16] M.-C. Timar, L. Gurau, M. Porojan, and E. Beldean, "Microscopic identification of wood species an important step in furniture conservation," *European Journal of Science and Theology*, vol. 9, no. 4, pp. 243–252, 2013.
- [17] N. Rosa da Silva, M. De Ridder, J. M. Baetens, J. Van den Bulcke, M. Rousseau, O. Martinez Bruno, H. Beeckman, J. Van Acker, and B. De Baets, "Automated classification of wood transverse cross-section micro-imagery from 77 commercial central-african timber species," *Annals of forest science*, vol. 74, pp. 1–14, 2017.
- [18] A. R. de Geus, S. F. d. Silva, A. B. Gontijo, F. O. Silva, M. A. Batista, and J. R. Souza, "An analysis of timber sections and deep learning for wood species classification," *Multimedia Tools Appl.*, vol. 79, p. 34513–34529, dec 2020.
- [19] V. Stagno, F. Egizi, F. Corticelli, V. Morandi, F. Valle, G. Costantini, S. Longo, and S. Capuani, "Microstructural features assessment of different waterlogged wood species by nmr diffusion validated with complementary techniques," *Magnetic Resonance Imaging*, vol. 83, pp. 139–151, 2021.
- [20] X. J. Tang, Y. H. Tay, N. A. Siam, and S. C. Lim, "Mywood-id: Automated macroscopic wood identification system using smartphone and macro-lens," in *Proceedings of the 2018 International Conference on Computational Intelligence and Intelligent Systems*, pp. 37–43, 2018.
- [21] R. Damayanti, E. Prakasa, L. Dewi, R. Wardoyo, B. Sugiarto, H. Pardede, Y. Riyanto, V. Astutiputri, G. Panjaitan, M. Hadiwidjaja, *et al.*, "Lignoindo: image database of indonesian commercial timber," in *IOP Conference Series: Earth and Environmental Science*, vol. 374, p. 012057, IOP Publishing, 2019.
- [22] G. Figueroa-Mata, E. Mata-Montero, J. C. Valverde-Otárola, D. Arias-Aguilar, and N. Zamora-Villalobos, "Using deep learning to identify costa rican native tree species from wood cut images," *Frontiers in Plant Science*, vol. 13, p. 211, 2022.
- [23] D. A. Cano Saenz, C. F. Ordoñez Urbano, H. R. Gaitan Mesa, and R. Vargas-Cañas, "Tropical wood species recognition: A dataset of macroscopic images," *Data*, vol. 7, no. 8, p. 111, 2022.
- [24] H. M. Lee, W.-S. Jeon, and J.-W. Lee, "Analysis of anatomical characteristics for wood species identification of commercial plywood in korea," *Journal of the Korean Wood Science and Technology*, 2021.
- [25] P. L. P. Filho, L. S. Oliveira, S. Nisgoski, and A. S. Britto, "Forest species recognition using macroscopic images," *Machine Vision and Applications*, vol. 25, pp. 1019–1031, 2014.
- [26] Y. Sun, "Wood Recognition." <https://github.com/sunyongke/woodRecognition>, 2020. [Online; accessed 02-March-2023].